

See discussions, stats, and author profiles for this publication at: <https://www.researchgate.net/publication/234065303>

Axial Flux Permanent Magnet Generator Design for Low Cost Manufacturing of Small Wind Turbines

Article in *Wind Engineering* · December 2012

DOI: 10.1260/0309-524X.36.4.411

CITATIONS

27

READS

8,345

4 authors:



Kostas Latoufis

National Technical University of Athens

24 PUBLICATIONS 160 CITATIONS

[SEE PROFILE](#)



Georgios Messinis

National Technical University of Athens

23 PUBLICATIONS 221 CITATIONS

[SEE PROFILE](#)



Panos Kotsampopoulos

National Technical University of Athens

65 PUBLICATIONS 950 CITATIONS

[SEE PROFILE](#)



Nikos D. Hatzigiorgiou

National Technical University of Athens

668 PUBLICATIONS 25,749 CITATIONS

[SEE PROFILE](#)

Some of the authors of this publication are also working on these related projects:



Distributed Energy Resources Research Infrastructure (DERri) [View project](#)



Locally Manufactured Small Wind Turbines [View project](#)

Axial Flux Permanent Magnet Generator Design for Low Cost Manufacturing of Small Wind Turbines

by

K.C. Latoufis, G.M. Messinis, P.C. Kotsampopoulos and N.D. Hatziargyriou

REPRINTED FROM

WIND ENGINEERING

VOLUME 36, No. 4, 2012

MULTI-SCIENCE PUBLISHING COMPANY
5 WATES WAY · BRENTWOOD · ESSEX CM15 9TB · UK
TEL: +44(0)1277 224632 · FAX: +44(0)1277 223453
E-MAIL: mscience@globalnet.co.uk · WEB SITE: www.multi-science.co.uk

Axial Flux Permanent Magnet Generator Design for Low Cost Manufacturing of Small Wind Turbines

K.C. Latoufis¹, G.M. Messinis¹, P.C. Kotsampopoulos¹ and N.D. Hatzargyriou¹

¹National Technical University of Athens (NTUA), Iroon Politechniou 9, Zografou, Athens, Greece.

Email: latoufis@power.ece.ntua.gr

Submitted July 25, 2011, Revised July 5, 2012, Accepted July 6, 2012

ABSTRACT

In this paper the design and manufacturing processes for coreless axial flux permanent magnet generators are described for low cost rural electrification applications, where local production of small wind turbines is considered. The process is based on already existing open source design and construction manuals, while a systematic approach to designing generators of varying nominal power and for grid connection or direct battery charging schemes is described. The manufacturing process of a 3 kW small wind turbine generator for grid connection is used as a case study. Emphasis is given to the use of simple tools and techniques to achieve a lower cost, while intricate steps in the manufacturing process are described in more detail. The generator design is simulated and the constructed machine is tested in the laboratory.

Keywords: Axial flux, low cost applications, open source hardware design, permanent magnets, rural electrification, small wind turbines.

List of symbols

α_i	pole arc to pole pitch ratio
B_{mg}	magnetic flux density on magnet surface (T)
B_p	peak value of the fundamental component of airgap flux density (T)
B_r	remanent magnetic flux density (T)
$C_{p_{max}}$	maximum power coefficient
C_q	heat coefficient (W/cm ²)
d_c	copper diameter (mm)
D_{in}	generator inner diameter (mm)
D_{out}	generator outer diameter (mm)
E_f	electro-magnetic force (V)
f_{nom}	generator nominal frequency (Hz)
g	mechanical clearance gap (mm)
H_c	coercive field strength (A/m)
h_m	permanent magnet thickness (m)
h_r	back iron thickness (m)
I_{ac}	nominal AC current (A)
$I_{ac_{max}}$	maximum AC current (A)
J_{max}	maximum current density (A/mm ²)
k_d	inner to outer radius ratio
k_f	coil fill factor

k_{sat}	saturation factor
l_a	active length (m)
l_{avg}	average coil length (m)
l_{ec}	end-turn length (m)
L_s	generator inductance (mH)
n	generator RPM
N_c	number of turns per coil
n_{nom}	nominal RPM
N_{phase}	number of turns per phase
p	number of pole pairs
P_{air}	aerodynamic power (W)
P_{nom}	generator nominal power (W)
P_{cu}	ohmic losses (W)
ρ_{cu}	copper density (kg/m ³)
q	number of coils per phase
Q	total number of coils
R_c	coil resistance (Ω)
R_{in}	inner radius (m)
R_{out}	outer radius (m)
R_{turb}	wind turbine diameter (m)
sc	copper crosection (mm ²)
S_{PM}	permanent magnet surface area (m ²)
t_w	stator axial thickness (m)
v_w	wind speed (m/s)
w_c	coil side width (m)
w_m	permanent magnet radial width (m)
η	generator efficiency
λ_{opt}	optimum tip speed ratio
μ_0	vacuum permeability (Wb/(A·m))
μ_{rrec}	recoil permeability
ρ	air density (kg/m ³)
ρ_{cu}	electrical resistivity of copper (Ω m)
Φ_{max}	maximum magnetic flux (Wb)
ω_e	electrical speed (elec.radians)

I. INTRODUCTION

In small scale residential or rural applications, the use of small wind turbines for the production of electricity is a common practice, when connection to the grid is not an option or when favourable feed in tariffs exist. Small wind turbines have a wide range of nominal power values reaching up to 88 kW [1] and frequently use permanent magnets to produce the generator's excitation field. The use of permanent magnets in a coreless axial flux generator makes the construction process easier and suitable for locally manufactured open hardware wind power applications. Such generators have often been studied in literature [2], [3] and the construction process is openly documented in detail in [4], resulting in the use of many small wind turbines of this type in rural electrification applications throughout the world. Using these designs as a basic platform, along with some simple theoretical equations, the generator can be designed and manufactured according to the nominal power needed, in any small scale application. In this paper, a description of these basic theoretical concepts and construction

methods is presented, while a 3 kW generator is constructed and tested in the laboratory to verify the proposed analysis.

2. WIND TURBINE CONNECTION SCHEMES

In the initial steps of the design process, the type of connection to be realised must be considered. The two possible options outlined in this paper, which are the most frequently used applications, are direct battery charging and grid connection. The small wind turbine construction procedure is the same in both direct battery charging and grid connection schemes, but some different design requirements need to be considered.

Direct battery charging applications [5], are usually preferred at a household or small business level in the rural context, due to lower initial costs, and also when connecting to the utility grid is not an option or is an insecure option due to power cuts or load shedding. The generator output will be rectified through an uncontrolled full wave diode bridge rectifier and then fed to the battery bank (Figure 1). When the turbine's rotor blades start rotating, the generator output voltage V_{cut-in} must be equal to the batteries' voltage V_{batt} i.e. $V_{cut-in} = V_{batt}$. This happens when the wind rises to the cut-in wind speed $v_{wcut-in}$. This wind speed is frequently set at 3 m/s for rural and residential applications, both in open source hardware designs as in [4] and in commercial wind turbine designs. It must be noted though, that after testing locally manufactured wooden rotor blades and commercial rotors in small wind turbine test sites, it has been observed that the rotor needs an initial wind gust of higher wind speed to start rotating [6]. From this point onwards and once rotation has commenced, the small wind turbine can produce power for winds higher than 3 m/s. Thus, the cut-in voltage is the only restriction in the design of a generator for direct battery charging.

The connection to the grid is slightly more complex. In order to be able to realize a grid connection, access to some form of grid with stable and specific voltage and frequency levels, is necessary. This could be the main low voltage distribution grid or a local microgrid [7]. In the first case a wind turbine could feed power to the utility grid and take advantage of some sort of feed-in tariff. In the second case, many small wind turbines or other micro sources can be interconnected in the AC bus of a microgrid structure making a more efficient use of energy and allowing for more spatial dispersion of the micro sources. The microgrid architecture uses a central control inverter, namely the battery inverter who can satisfy any kind of load up to its nominal power through its connection to batteries, and has the capability of synchronization to the main power grid or to a diesel generator. Considering the small wind turbine design in the case of grid connection, the generator output is rectified through an uncontrolled full wave diode bridge rectifier and then fed to a grid-tie inverter (Figure 2). The inverter's DC input voltage range V_{Low} to V_{High} is a restriction to the design procedure. This input voltage range is protected by the overvoltage protection device, which uses a dump load resistor in order to keep input voltages always in the specified range. The voltage of the generator needs to vary in this range and the cut-in voltage V_{cut-in} must be at least equal to V_{Low} . At the nominal wind speed of v_{wnom} , which is characterized as the wind speed after

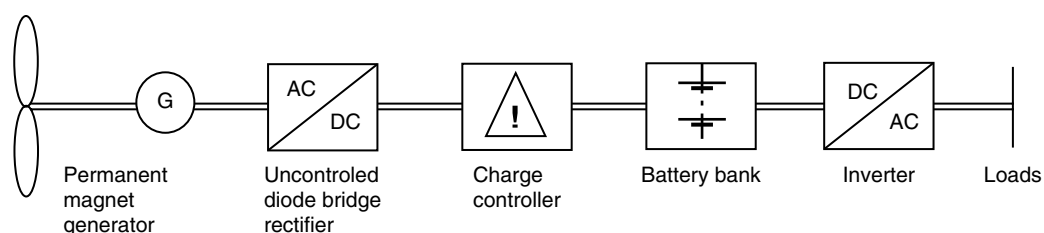


Figure 1: Block diagram of a direct battery charging scheme.

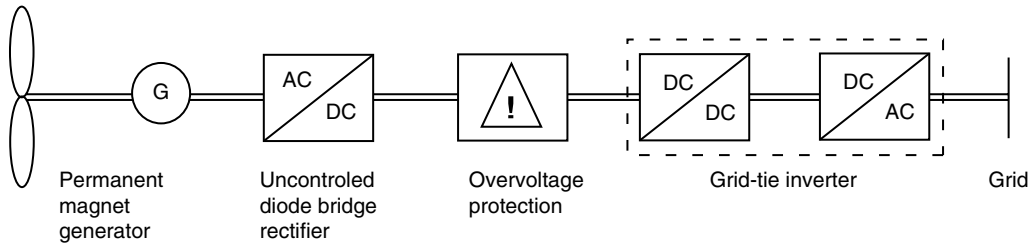


Figure 2: Block diagram of a grid connection scheme.

which the furling tail aerodynamic braking system starts to function and also the wind speed at which the generator produces its nominal power, the generator's voltage output must not be higher than V_{High} . This wind speed is usually set at 10 m/s [8] for rural applications.

A great advantage of using an inverter designed for grid connected small wind turbine applications is the capability of the maximum power point (MPP) operation. This operation provides maximum power output for every wind speed, by keeping both the tip speed ratio constant at its optimum value λ_{opt} and the aerodynamic power coefficient at its maximum value $C_{p_{max}}$. The values of λ and C_p are special characteristics of the rotor blades' design and for most of the designs described in [4], are set at $\lambda_{opt} = 7$ and $C_{p_{max}} = 0.35$.

Finally, it must be noted that a grid connection would produce more energy over time, against the direct connection to a battery bank. This is due to the grid-tie inverter's DC/DC converter which runs the MPP algorithm, in order to drive the generator over a wide range of voltages and thus operate the turbine in optimal λ conditions, producing more energy. In the case of the direct battery connection, the battery voltage, which has a limited range, keeps the generator voltage low, which eventually slows down the rotor blades. In this case the rotor blades will not be able to operate in optimal λ conditions and thus less energy will be produced in time. A comparison of the two connection schemes could be made in outdoor field tests, when comparing the annual energy production of the two cases. It must be noted that MPP tracking also exists for direct battery charging systems, but it is not a very common application due to increased costs.

As a conclusion, examples for the design procedure of a 3 kW at 10 m/s small wind turbine generator for direct battery charging and grid connected schemes, are presented in the next sections.

2.1. Direct battery charging

Assuming a battery voltage of $V_{batt} = 48 \text{ VDC} = V_{cut-in}$ and given that the wind turbine operates between wind speeds of $v_{wcut-in} = 3 \text{ m/s}$ and $v_{wnom} = 10 \text{ m/s}$, other generator characteristics can be calculated. In the case of direct battery charging the tip speed ratio is not constant, but decreases as the wind speed increases, due to lower voltages in the stator that limit the rotational speed of the generator's rotor and thus slow down the rotor blades. In order to achieve the optimum value of λ at a typical average wind speed for rural applications of about 4-5 m/s, the tip speed ratio is set at $\lambda_{cut-in} = 8.75$ [4] for the cut-in wind speed. Assuming a $\eta = 90\%$ [9] generator efficiency during nominal conditions and given the nominal power output P_{nom} to be 3 kW, the turbine radius R_{turb} can be calculated. Setting $C_p = 0.35$ for λ_{opt} at nominal wind speed v_{wnom} the aerodynamic power is $P_{air} = P_{nom}/\eta$, where η is the generator efficiency. With the use of Equation (1), where the air density at sea level is $\rho = 1.2 \text{ kgr/m}^3$, the turbine rotor radius can be calculated to be $R_{turb} = 2.25 \text{ m}$.

$$R_{turb} = \sqrt{\frac{2P_{air}}{\pi\rho C_p v_w^3}} \quad (1)$$

Using the definition of the tip speed ratio in (2), and replacing for $\lambda_{cut-in} = 8.75$ at $v_{wcut-in} = 3$ m/s and for $\lambda_{opt} = 7$ at $v_{wnom} = 10$ m/s, the working range for n (RPM) of the generator can be calculated as $n_{cut-in} = 111$ RPM and $n_{nom} = 297$ RPM.

$$\lambda_{opt} = \frac{\omega R_{turb}}{v_w} = \frac{2\pi n R_{turb}}{60 v_w} \rightarrow n = \frac{60 v_w \lambda_{opt}}{2\pi R_{turb}} \quad (2)$$

Finally the generator's voltage working range can be calculated. The DC voltage V_{dc} at cut-in must be equal to $V_{batt} = 48$ V plus the 1.4 V voltage drop across the rectifier which is a more significant percentage of the generator's cut-in voltage in lower voltage systems like a 24 VDC or a 12 VDC system. So the respective AC voltage V_{ac} before the uncontrolled diode bridge rectifier should be equal to 21.12 V according to (3) and this voltage is equal to the EMF voltage at cut-in $E_{fcut-in}$ since the wind turbine is in open circuit. The nominal EMF voltage E_{fnom} can then be calculated from (4):

$$V_{batt} = \sqrt{3} \cdot 1.35 \cdot V_{ac} - 1.4 \quad (3)$$

$$\frac{E_{fnom}}{E_{fcut-in}} = \frac{n_{nom}}{n_{cut-in}} \rightarrow E_{fnom} = \frac{n_{nom}}{n_{cut-in}} E_{fcut-in} \rightarrow E_{fnom} = 56.51 \text{ V} \quad (4)$$

At this point it must be noted that the nominal power of the generator will never be reached at the nominal wind speed of 10 m/s, when connected directly to a battery bank. The value of the tip speed ratio λ will not be optimal, since the rotor blades will be stalled because of the low voltage connection to the batteries. Thus, the aerodynamic coefficient C_p will be significantly less than 0.35 and the nominal EMF voltage E_{fnom} will never be reached at this wind speed. A practical way to overcome this disadvantage, is to choose an appropriately high resistance in the copper cable which connects the generator to the battery bank. This will provide an adequate voltage drop on the cable, which will in turn raise the generator's voltage working range and thus its tip speed ratio in higher wind speeds. This approach is useful as long as the generator's cut-in wind speed remains reasonably close to 3 m/s.

2.2. Grid connection

It has already been stated that when operating in grid connection and with a MPP controller, the tip speed ratio is kept constant at its optimum value at all times ($\lambda_{opt} = 7$ for the rotor described in this paper), except during cut-in when the generator is in open circuit and operates with $\lambda_{cut-in} = 8.75$. Considering a standard 3 kW inverter with DC input range of 200-500 VDC and using (3) the calculation procedure is as follows:

$$E_{fcut-in} = \frac{200}{\sqrt{3} \cdot 1.35} = 85.5 \text{ V} \quad (5)$$

$$E_{fnom} = \frac{500}{\sqrt{3} \cdot 1.35} = 213.8 \text{ V} \quad (6)$$

At the nominal wind speed of 10 m/s and for $\lambda_{opt} = 7$ the nominal RPM is found $n_{nom} = 297$ RPM using (2), and the cut-in RPM can then be calculated. This kind of RPM corresponds to a cut-in wind speed given by (8).

$$\frac{E_{fnom}}{E_{fcut-in}} = \frac{n_{nom}}{n_{cut-in}} \rightarrow n_{cut-in} = \frac{E_{fcut-in}}{E_{fnom}} n_{nom} \rightarrow n_{cut-in} = 119 \text{ RPM} \quad (7)$$

$$v_{wcut-in} = \frac{2\pi n_{cut-in} R_{turb}}{60\lambda_{opt}} = 3,2 \text{ m/s} \quad (8)$$

At this point it can be noted that the commercial grid-tie inverter that has been chosen in this example, limits the working range of wind speeds for grid connection (3.2-10 m/s), with respect to those of direct battery charging (3-10 m/s). This is not a general conclusion, but the design for the grid connection could alternatively have been done with the goal of achieving a cut-in voltage at a wind speed of 3 m/s. In this case though, the wind turbine would not be able to produce its nominal power since the voltage produced at nominal wind speed would exceed the inverter's maximum DC input voltage. Thus, either another commercial inverter with a wider DC input voltage range would be needed or a grid-tie inverter would be designed for the specific generator's voltage operating range, as is done for many commercial small wind turbines in the market. Returning to the analysis, despite the possibility of operating with a slightly limited wind speed range during grid connection, working on the MPP will result in higher energy production. The resulting conclusion is that the grid-tie inverter's DC input voltage range must be carefully chosen to match the generator's voltage range and the required wind speed range of operation for the application in question.

3. CHOOSING THE GENERATOR FREQUENCY, POLE PAIRS AND COIL NUMBER PER PHASE

Since the generator output voltage will be rectified, choosing a specific nominal frequency will be more relevant to the total cost of the generator than its operational characteristics. This is due to the fact that the nominal frequency f_{nom} (i.e. the frequency at nominal wind speed) determines the number of poles pairs p given by (9) and thus the total number of magnets. The permanent magnets used in these designs are rectangular neodymium magnets (NdFeB) which are the most expensive and rare material used in the construction process of this small wind turbine. Thus, reducing the number of pole pairs will reduce the overall cost of the generator. Nevertheless, according to literature [10], there are cases when the reduction of the number of pole pairs results in reduced efficiency and distorted voltage waveforms and harmonics. In this design approach the nominal frequency is set to 50 Hz.

In general, mounting the magnets close to one another is preferred if possible, but this aspect of the generator's design will not be considered in this paper. The parameter that defines this aspect is the magnet width (pole arc) to pole pitch ratio a_i and values between 0.4 and 0.7, seem to be suitable for the applications in question.

$$p = \frac{120f_{nom}}{n_{nom}} \quad (9)$$

$$\frac{2Q}{3p} = 0.5 \quad (10)$$

The coils are connected in a three phase system using a star connection. The coil number Q can be calculated from (10) [11] and thus the proper pole pair to coil combinations for creating a three phase system, are presented in Table 1.

Table 1: Pole-coil combinations

8	6	12	9	16	12	20	15	24	18	28	21
---	---	----	---	----	----	----	----	----	----	----	----

4. THE GENERATOR AXIAL DIMENSIONS

The axial dimensions of the generator (Figure 3) include the thickness of the back iron rotor disks, the thickness of the magnets h_m , the mechanical clearance gap g and the thickness of the stator t_w . Having chosen the most cost effective commercial magnets to be found that are suitable for this application and are used in [4], their thickness and grade are set and are $h_m = 10$ mm and grade N40, while their other dimensions are 30 mm width and 46 mm length. The mechanical clearance gap g is chosen at 3 mm and consists of a 1 mm mechanical gap, 1 mm of resin over the magnets and 1 mm of resin over the stator coils. A reduction in the total air gap could be achieved by minimizing the thickness of the resin layer over the magnets and the stator, resulting in higher induced voltages and higher power outputs. The resin layer over the neodymium magnets should not be eliminated though, because it protects them from corrosion (Figure 5), especially in marine environments. Also the gradual degradation of the bearing needs to be taken into account resulting in possible future misalignments of the bearing shaft that might cause friction between the stator and the rotor disks. In this case a larger mechanical clearance gap would prevent this from being a problem and would produce a more robust generator. An increase in the mechanical clearance gap without a reduction in produced power could be achieved with the use of slightly stronger magnets i.e. of grade N42.

The axial thickness of the stator coils can be calculated by (11) [9], which results from the analysis of the magnetic circuit while assuming no magnetic flux density leakage. The magnetic flux density near the magnet's surface B_{mg} is usually set at about $B_r/2$, where the remanent magnetic flux density B_r and coercive field strength H_c are characteristic values of the magnet that are related to its grade and can be easily extracted from neodymium magnet data sheets. Other variables are $k_{sat} = 1$ due to the coreless stator and μ_0 the vacuum permeability.

$$B_{mg} = \frac{B_r}{1 + \mu_{rec} \frac{(g + 0.5t_w)}{h_m} k_{sat}} \quad (11)$$

$$\mu_{rec} = \frac{1}{\mu_0} \frac{B_r}{H_c} \quad (12)$$

If NdFeB N40 magnets are chosen then Equation (11) can be rewritten for the thickness of the stator as:

$$t_w + 2g = 2h_m \rightarrow t_w = 2h_m - 2g \quad (13)$$

Finally, the thickness of the back iron disks is complex to calculate from theoretical equations and has been studied in literature only with the use of finite element modeling methods [12]. Some general characteristics of the back iron disks can be stated though. The back iron disk thickness should be reduced as much as possible in order to avoid increases in the total weight of the generator, but at the same time it should not be reduced too much in order to withstand the attractive magnetic forces pulling the two rotor disks together and thus ruining the mechanical clearance gap and damaging the generator. Also, magnetic saturation is possible in the iron disk if it is chosen too thin. A practical "rule of thumb" states that the back iron thickness should be equal to the magnet's thickness. The attractive forces between the rotor disks are the main factor that influences the back iron thickness. A way to minimize those forces is to retain a low magnet width to pole pitch ratio a_i together with a high inner to outer radius ratio k_d during the design phase of the generator. This combination actually results in magnet poles with less active surface area and thus reduced attractive forces.

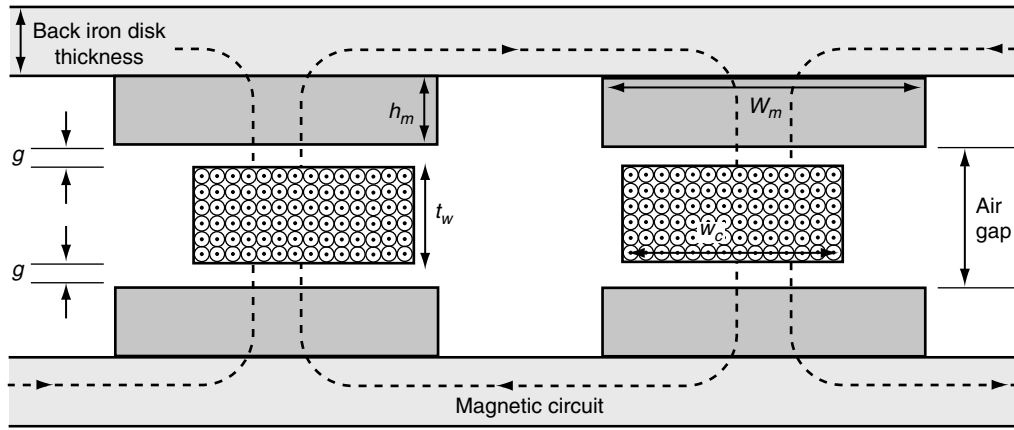


Figure 3: Axial dimensions of the generator (rotor disks and magnets, stator coils and clearances)

5. THE GENERATOR WINDING DIMENSIONS

Using basic equations for electromagnetic induction and assuming an almost sinusoidal magnetic flux density B , the required turns per coil can be calculated in a simplified way. Initially, the maximum flux per pole Φ_{\max} is calculated using (14):

$$\Phi_{\max} = B_{mg} \cdot w_m \cdot l_a \quad (14)$$

where w_m is the magnet's width and l_a is the magnet's length and also the active length of the generator (Figure 4). Then the number of turns per coil N_c are calculated using (15), where k_w is a winding coefficient equal to 0.95, q is the number of coils per phase, n is the RPM at cut-in and E_f is the corresponding induced EMF voltage during cut-in:

$$N_c = \frac{\sqrt{2}E_f}{q \cdot 2\pi \cdot k_w \cdot \Phi_{\max} \cdot n \cdot p / 120} \quad (15)$$

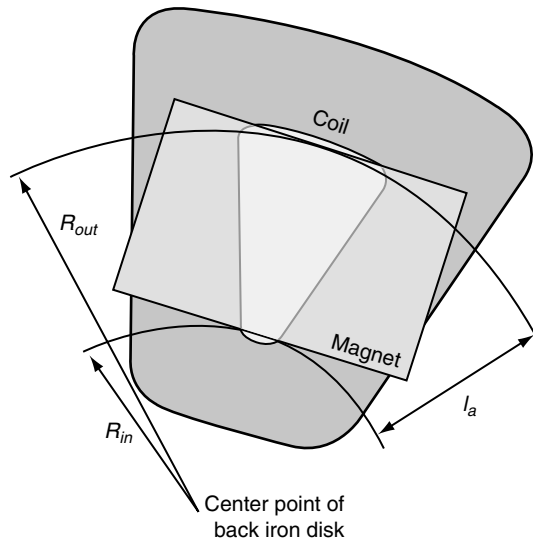


Figure 4: Inner radius, outer radius and active length of the generator.



Figure 5: The generator's rotor as it came out of the mould: Neodymium magnets cast in polyester resin.

Given the number of turns per coil N_c and the stator's axial thickness t_w , the coil leg width w_c is calculated in (16) for a value of the heat coefficient cq that is equal to 0.3 W/cm^2 [4] and where I_{acmax} is the maximum generator current and ρ is the electrical resistivity of copper.

$$w_c = \frac{I_{acmax} \cdot N_c}{\sqrt{\frac{2 \cdot cq \cdot k_f \cdot t_w}{\rho}}} \quad (16)$$

The fill factor of the coils, which signifies the ratio of copper area to the total area of a cross-section of a coil, is represented with k_f . A value close to 0.55 is adequate for this factor as far as manually constructed coils are concerned. Even higher values of k_f such as 0.7 can be achieved in manual construction (theoretical maximum $k_f = 0.78$ for conductors of circular cross-section), depending though on the shape of the coil, the number of coil turns and the copper conductor's diameter. A misjudgement on the estimation of the fill factor can cause serious construction problems especially in the case that the fill factor turns out to be lower than initially assumed, since the coils will not be able to fit in the stator mould. If k_f turns out to be higher than assumed, then this will not pose such a severe problem. The outcome will be a

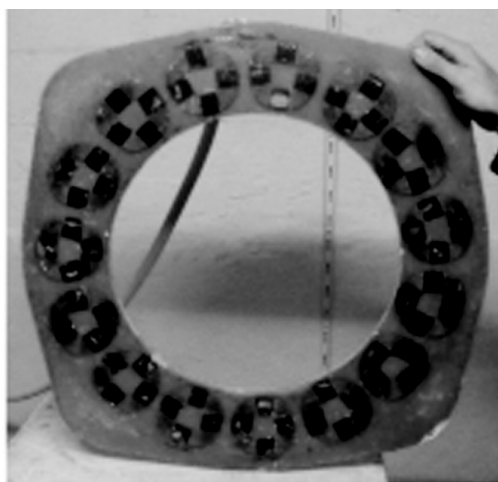


Figure 6: The generator's stator: Coils cast in polyester resin.

gap between the coils (Figure 6) which will lead to the ineffective usage of the generator's present volume and to difficulties in the symmetrical alignment of the coils in the stator mould, since the touching sides of the coils are a valuable guide for their proper alignment. Due to the reasons mentioned above, the coil to be used must be constructed before the design phase is completed, in order for the fill factor to be measured. If the measured fill factor is close to the predicted one, the design can be implemented. Else, the design process must be conducted once more.

Along with the heat coefficient cq , the maximum current density J_{\max} of the winding must be considered as shown in (18). This is given after calculating (17) for $I_{ac\max}$, where instead of I_{ac} which is the AC current of the generator for P_{nom} , $I_{ac\max}$ is used which is the maximum current produced momentarily in a wind gust of 10% more power than the nominal power P_{nom} . Then (19) needs to be calculated for the copper cross-sectional area s_c .

$$I_{ac\max} = \frac{1,1 \cdot P_{nom}}{3 \cdot E_{nom} \cdot \eta} \quad (17)$$

$$J_{\max} = \frac{I_{ac\max}}{s_c} \quad (18)$$

A standard approach for small wind turbine design would be a value for current density of 6 A/mm² without this value being restrictive. The structure of the generator, with the two rotating disks acting as fans and cooling the winding [13], [14] makes high values of current density possible.

Attention must be given when designing generators of larger power output i.e. larger than 2.5 kW. The generator's larger diameter prevents adequate circulation of air in the winding for cooling. The problem intensifies due to the lower RPM of the rotor disks due to larger rotor blade diameters. An improvement for air circulation is the drilling of large holes on the back iron disks [15] at radii smaller than the inner radius of the generator, while not neglecting to consider the attractive forces between the rotor disks that usually cause deflections closer to their centres [12]. It must be noted that variations of the fill factor will not have any impact on the current density J_{\max} , but on the contrary will effect the heat coefficient cq due to its dependence on the area of the coil's surface. Both cq and k_f must be calculated while designing a generator in order to avoid prolonged operation at temperatures which will overcome the thermal limits of the polyester resin in the stator.

The copper cross-sectional area S_c and the copper diameter d_c to be used are calculated from (19) and (20) respectively:

$$s_c = \frac{A_{reacopper}}{N_c} = \frac{k_f \cdot w_c \cdot t_w}{N_c} \quad (19)$$

$$d_c = \sqrt{\frac{4 \cdot s_c}{\pi}} \quad (20)$$

The terminal voltage of the generator at different RPM can be calculated with the use the (21) and (22) [9], for calculated values of resistance R_c and inductance L_s [5]:

$$\delta = \sin^{-1} \left(\frac{I_{rms} 2\pi f L_s}{E_f} \right) \quad (21)$$

$$V_t = E_f \cos \delta - I_{rms} q R_c \quad (22)$$

Concluding, the inner shape formed by each coil will be considered. According to [4] the coil's inner shape should have the same dimensions as the shape of the magnets. This is a good design approach and a "rule of thumb" process, if other design parameters of the generator such as the magnet width to pole pitch ratio a_i and the inner to outer radius ratio k_{db} will not be considered in the design procedure. This approach results in an improvement of the induced EMF waveform making it more sinusoidal, despite the value of a_i chosen in the design. This occurs due to a more gradual variation of the flux linkage. In the designs of [4] the magnet width to pole pitch ratio a_i has a value close to 0.4, which is quite low when compared to $a_i = 2/\pi$ [9] which produces sinusoidal EMF waveforms, yet the voltage waveforms are improved by matching the coil's inner dimensions to the dimensions of the magnets, as stated earlier. Consequently, the outer dimensions of the coils are also rectangular resulting in the use of single layer concentrated non overlapping windings.

Nevertheless, it is observed that this kind of winding does not fully exploit the generator's volume. A better usage of the generator's volume could be achieved by using trapezoidal coils (Figure 6) i.e. a double layer concentrated non overlapping winding [9], thus filling with copper the maximum possible volume of the stator. The resulting flux linkage is greater and thus the voltage induced and power produced are increased for the same volume of the generator. Or alternatively the total volume and weight of the generator could be reduced for the same nominal power. Rectangular magnets can still be used while considering that the magnet width to pole pitch ratio a_i is kept close to 0.6, which will produce waveforms that are close to sinusoidal.

Several times in this paper there has been reference to the quality of the generator's output waveforms. Current harmonics are frequently responsible for the production of losses in the form of acoustic noise and vibrations while the generator is operating.

Yet, connecting the generator to an uncontrolled diode bridge rectifier will inevitably degrade the output waveforms (Figure 8) and increase their harmonic content to such a degree, that achieving a sinusoidal EMF (Figure 7) while designing the generator, will probably have no significance in the performance of the small wind turbine system.

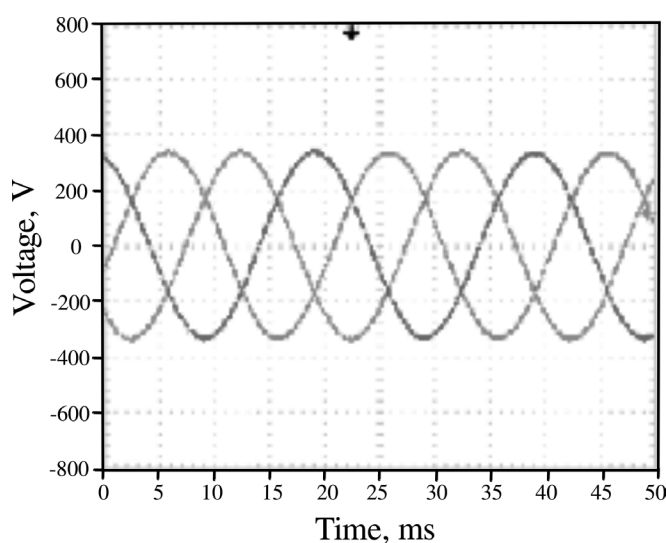


Figure 7: The terminal line-to-neutral voltage of phases A, B and C under a symmetrical three phase ohmic load in star configuration.

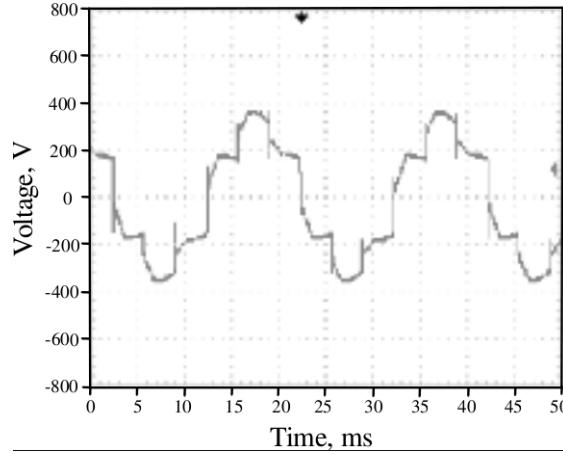


Figure 8: The terminal line-to-neutral voltage of phase A when connected to an uncontrolled diode bridge rectifier and an ohmic load.

6. THE GENERATOR OUTER RADIUS

Using all previously calculated variables, the inner and outer diameter of the generator, and thus the outer diameter of the back iron disks (Figure 4), can be calculated. Initially the inner diameter is calculated in a geometrical manner and then the outer diameter is calculated simply by adding the active length of the generator. The inner and outer diameters of the generator are calculated in (23) and (24):

$$R_m = \frac{2Q \cdot w_c + p \cdot w_m}{2\pi} \quad (23)$$

$$D_{out} = D_{in} + 2 \cdot l_a \quad (24)$$

An additional factor when designing a generator for local construction with simple manufacturing processes and for low cost, has to do with the outer diameter. As the outer diameter increases simple and inexpensive ways to cut the rotor disks result in uneven iron disks. In the 3 kW generator design described later in this paper, with rotor iron disks of 240 mm radius and 10 mm thickness, it was found that the two disks were not totally plane and thus parallel to each other, but were slightly bent, resulting in poor mechanical clearance gap regulation, and thus reduction of the expected nominal power. This was the result of cutting the back iron disks with a plasma pantograph router in order to reduce costs and to avoid the usage of complex machinery, such a lathe to make the two disks plane. More sophisticated ways of cutting the iron rotor disks such as CNC laser could be used, while increasing the total cost for the generator. A further restriction to the outer diameter of the generator concerns the drill press. This common workshop tool is used in many low cost construction applications in order to drill holes on the rotor iron disks, from which thread rods will pass that join the turbine's rotor blades and rotor disks to the bearing hub and shaft. The rotor disks need to fit in the drill press otherwise the holes will need to be drilled with a hand drill, thus increasing not only the construction time but also the possibilities of misalignment, due to difficulties in centring the bearing hub on the rotor disks.

7. THE MANUFACTURING PROCESS

All the issues analysed previously are mainly concerned with the design process of the generator, while emphasis is given at specific points that need to be considered in order to complete the construction phase without any major problems. This section is dedicated to issues arising during the manufacturing process.

7.1. Winding coils

The construction of the generator begins with constructing the coil winding tool (Figure 9). This simple tool is made from wood and threaded rods, as described in [4] and consists of three parts. Two outer disks and an inner piece, the spacer. The spacer sets the axial thickness t_w of the coils and thus of the stator. In order for the constructed coils to have the exact axial thickness that was previously calculated, the spacer needs to be cut 1 mm thinner than calculated, because the coils tend to expand slightly when they are removed from the winding tool. In this manner, technical problems can be avoided in the regulation of the mechanical clearance gap during the assembly of the generator, while keeping the air gap at the calculated length.

For winding the coils it is essential to carefully count the turns, to make sure one turn of copper conductor is set next to the other and to tense the conductor enough, as this results in less gaps in between the turns of copper conductors and thus more successful coils. The fill factor must be measured at this stage in order to verify the design procedure mentioned in earlier chapters.

7.2. Constructing moulds

Construction difficulties concerning the building of the stator and the stator's moulds are not likely to occur. A slight slope must be given to the inside side walls of all moulds (Figure 10). This will help removing the rotor and stator polyester resin parts after casting, without damaging them or having to dismantle the moulds.

7.3. Rotor magnet disks

Great attention must be given to the magnet positioning piece (Figure 11). The process described in Hugh Piggott's "Small Wind Turbine Recipe Book" [4] is very accurate, but still there might be some confusion that may cause important errors, especially if a new design is constructed. It must be kept in mind that after mounting the magnets, the two rotor disks will

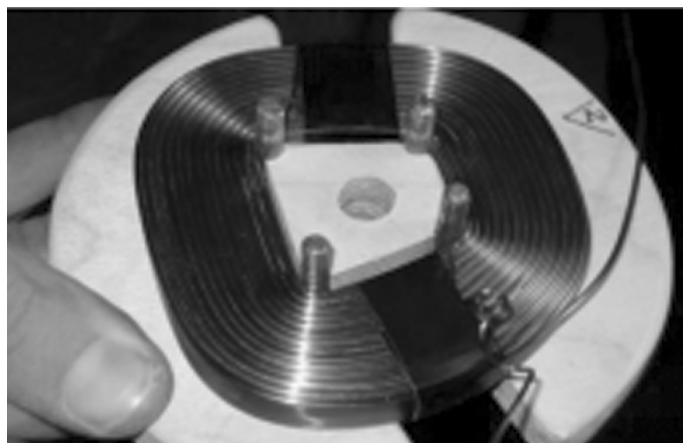


Figure 9: A properly constructed coil still on the hand tool.

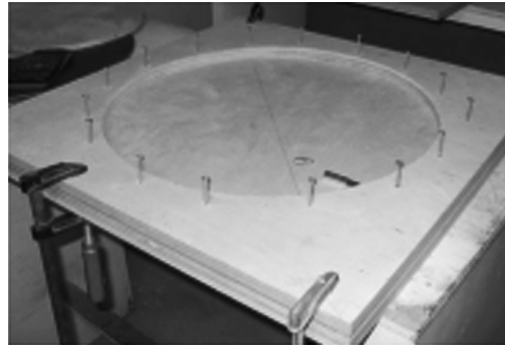


Figure 10: The rotor disk mould. A slight slope is given to the side walls of all moulds.

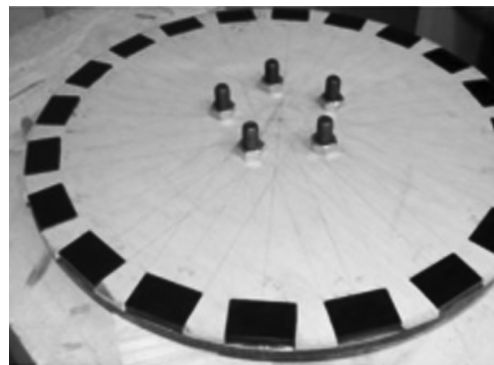


Figure 11: The magnet positioning piece. All magnets are positioned with the correct polarities on the first rotor disk.

be facing each other and in this position each magnet will face a magnet of opposite polarity, so that the two disks attract each other and thus create the required magnetic circuit. In order to avoid misalignment of the rotor magnet disks, one of the threaded rod holes on the rotor must be marked and the centre of a magnet must be aligned to that hole, making it the index hole.

If for some reason this is not possible, then the magnet positioning piece needs to be turned over when mounting the magnets on the second disk. When manufacturing a new generator design, with different pole pair numbers, accuracy and caution will be needed when dealing with this specific problem. A test run before mounting the magnets is the best practice to avoid mistakes (Figure 12).

7.4. Materials and tools

All the materials and tools used in the construction of a locally manufactured generator need to be easily sourced and at low costs.

The use of iron in order to construct the generator's metal frame and the use of plywood in order to construct the magnet positioning jig and the stator and rotor moulds, are ideal for low cost applications. These materials can be found anywhere and can be treated with low cost power tools found in metal and wood workshops, that do not require expert skills. The back iron disks need to be cut with a plasma pantograph router that can be found in large cities. Otherwise, they can be manufactured by hand, only to increase the overall labour time needed for the construction.



Figure 12: The magnet positioning piece was not correctly positioned on the second rotor disk, so new holes had to be drilled for the bearing mounting studs.

The bearing hub for the horizontal axis of rotation of the generator, is a car or trailer hub which can also be found in commercial centres of large towns. The same stands for copper wire with enamel, used for generator windings.

Finally, the use of neodymium magnets, which are stronger magnets for less volume when compared to ferrite magnets, and the use of polyester resin as a material that can provide support for the stator coils which lay in the air and protection from corrosion for the magnets, need to be discussed. These materials are reasonably easy to find. The magnets can be ordered through the internet or by phone and polyester resin is a common material used for the reparation of fishing boats which can be sourced easily in rural workshops. In the last years though, with the rising price of rare earth materials, there is an on going discussion whether neodymium magnets are becoming too expensive for these applications and if a return to ferrite magnets would be a solution. Additionally, polyester resin tends to develop cracks over time which might allow water to enter into the back iron disks of the rotors and thus accelerate corrosive processes, especially in marine environments. Galvanised back iron disks can decelerate corrosion and the use of vinyl ester resins can reduce shrinkage of the casting and create better adhesion to the magnets and the back iron disks.

8. THE 3 kW SMALL WIND TURBINE GENERATOR CASE STUDY

All design and construction issues mentioned in this paper were encountered while designing and constructing a small wind turbine generator of 3 kW nominal power. This generator was designed for a 4.34 m diameter rotor, which will produce its nominal power at a wind speed of 10 m/s, as mentioned in Section 2 of this article. The generator was designed for connection to the grid through an uncontrolled diode bridge rectifier and a grid-tie inverter with DC input voltage range of 200-700 VDC which resulted in $n_{nom} = 297$ RPM and $E_{fnom} = 286$ V and $n_{cut-in} = 89$ RPM and $E_{fcut-in} = 85.5$ V, with the use of the procedure described in Section 2.2. The maximum AC current I_{acmax} and the terminal voltage V_t for n_{nom} were calculated to be 4.27 A and 217 V, respectively by using the procedure described in Section 5.

Initially, a theoretical analysis was performed and then the design was simulated with the use of technical computing and finite element analysis (FEA) software. The scripts developed required basic programming skills, such as those required for the use of MATLAB, and the designed generator was simulated with the use of the open source software package Finite Element Method Magnetic (FEMM), which resulted in an overall, simple and low cost design process. The simulation results verified the theoretical analysis and so the generator was optimized for low cost and was manufactured using simple manufacturing techniques and

tools, always having in mind a rural application where the small wind turbine would be locally manufactured (Figure 13). The general characteristics of the constructed generator are shown in Table 2.

The overall cost of the generator, for material prices as of December 2010, amounted up to 668€, which implies a cost of 223 €/kW. This results in a significant reduction in the €/kW cost for the generator of the small wind turbine, since a common cost for generators in this nominal power range in the global market would amount up to 469 €/kW, from well established suppliers.

It must be noted though, that in the costs mentioned earlier, the total labor time of 280 unqualified man-hours has not been quantified in Euro. This is justified due to varying labor costs which depend on the location of construction. Additionally, the construction of the wind turbine could be realized voluntarily by the community that will actually use the small wind turbine, which is common practice in rural applications.

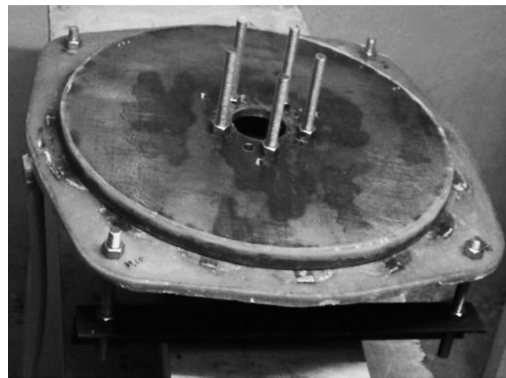


Figure 13: The constructed 3 kW small wind turbine generator.

Table 2: General characteristics of the 3 kW generator

<u>General Characteristics</u>		
Nominal power		3 kW
Nominal frequency		50 Hz
Pole pair number (p)		20
Coil number (Q)		15
Total cost		668 €
Cost/kW		223 €
Total mass		35.48 kg
Mechanical clearance (g)		3 mm
<u>Rotor</u>		
Rotor Iron Disks		
Thickness		10 mm
Outer radius (R_{out})		238.26 mm
Inner radius (R_{in})		207.05 mm
Inner/outer radius (k_d)		0.869
Magnets		
Axial thickness (h_m)		10 mm
Radial width (w_m)		46 mm
Active length (l_a)		30 mm
Pole arc/pole pitch (a_i)		0.659
<u>Stator</u>		
Coils		
Axial thickness (tw)		13.76 mm
Coil leg width (w_c)		31.54 mm
Turns per coil (N_c)		337
Conductor size (dc)		0.95 mm

8.1. Experimental results

As mentioned in previous parts of the paper, some of the major problems encountered during the manufacturing and design processes were: the large diameter of the rotor disks, in combination to the small drill press that was available, the misjudgement of the fill factor and the incorrect alignment of the magnets. This last mentioned issue made it mandatory to drill new holes on one of the rotor disks in order to correctly align the magnets. As far as the coils were concerned, the fact that their surface area was less than predicted due to a misjudgement of the fill factor and a resulting experimental increase in its value, resulted in difficulties in positioning symmetrically the coils.

The results of the construction and design issues mentioned above and their influence on the overall performance of the generator where tested under laboratory conditions (Figure 14). The generator was driven with a variable speed DC motor drive and initially connected to a three phase ohmic load in star configuration. The results were plotted in the following graphs: open circuit E_f vs RPM (Figure 15), line current (I_{ac}) vs RPM (Figure 16), power vs line current (I_{ac}) while varying the rotational speed from 30 RPM up to 300 RPM with a step of 30 RPM for every measurement and under a constant 107.46 Ω ohmic load (Figure 17) and terminal voltage vs line current (I_{ac}) (Figure 18). The percentage of deviation between the theoretical design's rated characteristics and the experimental values measured in the laboratory was calculated at 1.4% for the EMF, at 5.5% for the terminal voltage and at 5.5% for the rated power.

Further on, the generator's power output vs RPM was plotted by driving the generator under a constant 107.46 Ω ohmic load (Figure 19), which produced nominal power and current at 315 RPM.

The temperature in the generator was also slightly higher than expected due to the smaller coil surface area, but within the acceptable limits of the design procedure. Laboratory tests showed satisfactory thermal operation of the generator while producing nominal power for prolonged periods of time.

Regarding the operation of the generator, the EMF voltage was found to be slightly lower than expected and so was the output power at 297 RPM which was considered to be the nominal RPM. This resulted from poor mechanical clearance gap regulation caused by small deflections of the large rotor disks and also by the fact that the coils expanded by 1 mm when they were taken off the winding tool. Consequently the air gap length was slightly increased and resulted in weaker magnetic fields in the generator. Yet, the phase difference between each phase of the generator was measured to be 120° which implies a good layout of the coils in the stator.



Figure 14: Testing the generator in the laboratory with the use of a variable speed DC motor drive.

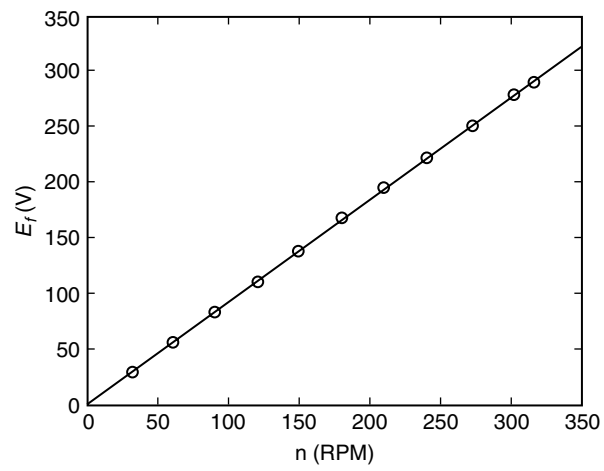


Figure 15: Electromotive force vs RPM.

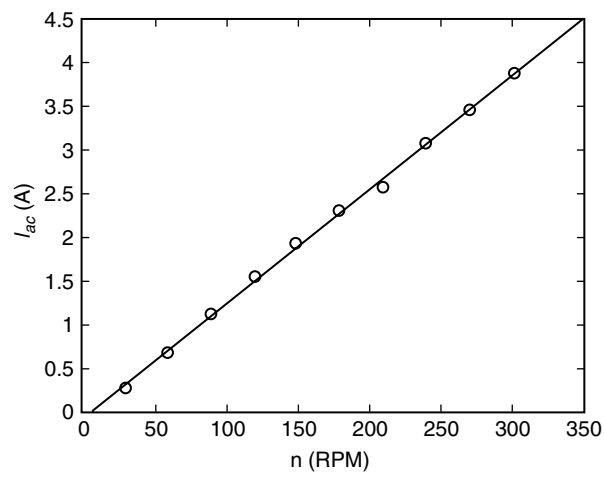
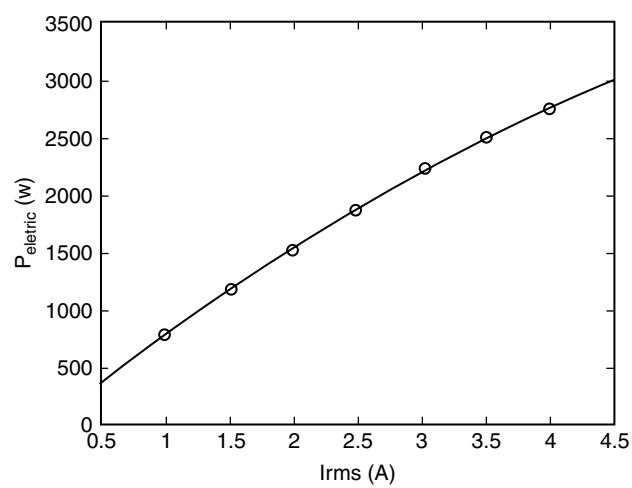
Figure 16: Line current vs RPM under a constant 107.46 Ω ohmic load.

Figure 17: Power vs line current.

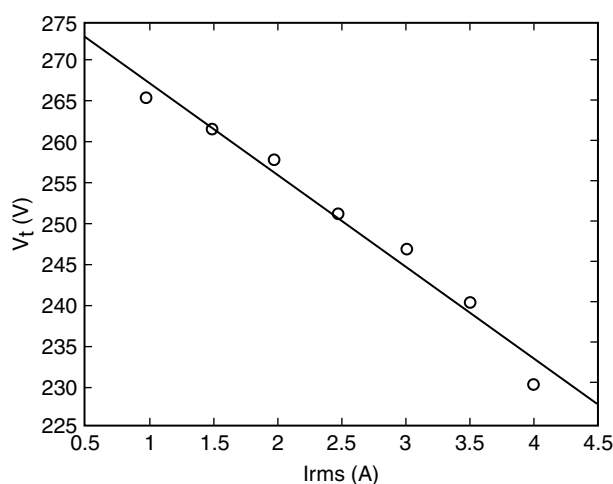


Figure 18: Terminal line-to-neutral voltage vs line current.

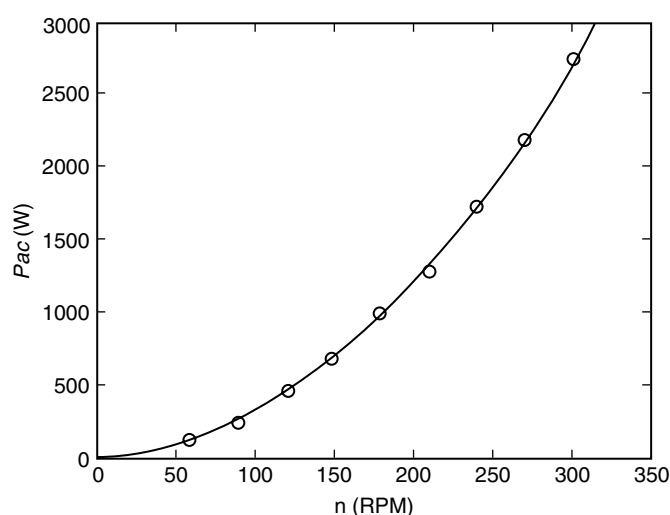


Figure 19: Power vs RPM.

When measured in open circuit operation, the generator run smoothly producing no acoustic noise or vibration. The same was observed when a symmetrical three phase ohmic load was connected at the output.

Further on, the generator was connected to a simply constructed uncontrolled diode bridge rectifier. There was some deviation from the theoretical equations describing the operation of uncontrolled diode bridge rectifiers and thus some deviation from the simulated output voltages.

Finally, some acoustic noise and vibrations were noted while loading the generator with an ohmic load through the rectifier (Figure 8), despite the fact that the design was conducted for almost sinusoidal EMF voltage waveforms. This was expected and is due to the harmonic distortion introduced to the system by the uncontrolled diode bridge rectifier.

9. CONCLUSION

An overview of the design and manufacturing processes of a 3 kW coreless axial-flux permanent-magnet generator for small wind turbines in rural electrification applications was made using basic theoretical tools, simple programming methods, partially open source software, and simple manufacturing techniques. These processes have proved to be easily

applicable while making transfer of such technological applications possible in the rural electrification context. These locally manufactured small wind turbines have proved to have robust designs and manufacturing processes. These processes can be easily understood with only basic scientific knowledge and also can be modified by the users and technicians that construct them to suit local needs and use local materials. These facts are the basis for the formation of open source hardware small wind turbines that can provide electrification for rural communities at a lower cost and empower local people with technical know-how on the manufacturing of renewable energy sources.

ACKNOWLEDGMENTS

The authors wish to thank Prof. D. Papantonis of the fluid dynamics laboratory of the mechanical engineering department of NTUA, for his support of this work by providing some of the components of the experimental set-up and all the students who assisted in the construction of the generator presented in this paper.

REFERENCES

- [1] *Wind Turbines-Part 2: Design Requirements for Small Wind Turbines*, CEI/IEC Std. 61400-2, 2006.
- [2] J.R. Bumby, N. Stanard, J. Dominy, and N. McLeod, "A Permanent Magnet Generator for Small Scale Wind and Water Turbines" in *Proc. of the 2008 International Conference on Electrical Machines*, paper 733, p. 1.
- [3] A. Parviainen, J. Pyrhonen and P. Kontkanen, "Axial Flux Permanent Magnet Generator with Concentrated Winding for Small Wind Power Applications" in *Proc. of the 2005 IEEE International Conference on Electric Machines and Drives*, p. 1187.
- [4] H. Piggott, *A Wind Turbine Recipe Book-The Axial Flux Windmill Plans*, 2009.
- [5] F.G. Rossouw, *Analysis and Design of an Axial Flux Permanent Magnet Wind Generator System for Direct Battery Charging Applications*, Msc Eng. thesis, University of Stellenbosch, South Africa, March 2009.
- [6] D.H. Wood, *Small wind turbines: Analysis, Design and Application*, 1st edition, Springer, 2011.
- [7] N.D. Hatziaargyriou, "Microgrids", *IEEE Power and Energy Magazine*, Volume 6, Issue 3, May-June 2008 Page(s): 26-29.
- [8] K.Christensen, *Catalogue of Small Wind Turbines*, Nordic Folkecenter for Renewable Energy, 2011.
- [9] J.F. Gieras, R.J. Wang and M.J. Kamper, *Axial Flux Permanent Magnet Brushless Machines*, 2nd ed. Springer, 2008.
- [10] M.J. Kamper, R.J. Wang and F.G. Rossouw, "Analysis and Performance Evaluation of Axial Flux Air-Cored Stator Permanent Magnet Machine with Concentrated Coils", *IEEE Transactions on Industry Application.*, vol. 44, pp. 1495-1504, 2008. (2002) The IEEE website.
- [11] M.V. Cistelecan and M. Popescu, "Study of the Number of Slots/Pole Combinations for Low Speed Permanent Magnet Synchronous Generators" in *IEMDC '07. IEEE International Electric Machines & Drives Conference, 2007, vol. 2, p. 1616*.
- [12] D.N. Mbidi, K. van der Westhuizen, R. Wang, M.J. Kamper and J. Blom, "Mechanical Design Considerations of a Double Stage Axial-Flux PM Machine", in *the Conference Record of the 2000 IEEE Industry Applications Conference*, vol. 1, pp. 198-201.

- [13] Rong-Jie Wang, *Design Aspects and Optimization of an Axial Field Permanent Magnet Machine with an Ironless Stator*, Ph.D. dissertation, University of Stellenbosch, South Africa, March 2003.
- [14] B.J. Chalmers and E. Spooner, "An Axial-Flux Permanent-Magnet Generator for a Gearless Wind Energy System", *IEEE Transactions on Energy Conversion*, vol. 14, no. 2, pp. 251-257, June 1999.
- [15] D. Bartmann, D. Fink, *Homebrew Wind Power: Hands-on guide to harnessing the wind*, Buckville Publications, 2009.

